

## Closing Remarks

### New Dimensions in Reaction Dynamics and Electronic Structure

**Dudley R. Herschbach**

*Department of Chemistry, Harvard University, Cambridge, Massachusetts 02138, U.S.A.*

The traditional functions of a Faraday Discussion: ‘to celebrate, to elucidate and to debate’, have again been amply fulfilled! I am grateful for the opportunity to give the customary benediction, on behalf of our newly inspired but now very tired clan. I welcome also this chance to express my own thanks for memorable meetings that over a span of more than thirty years have punctuated and accentuated the development of reaction dynamics.

Fig. 1 indicates the series of Discussions most directly antecedent to this one, each specified by year and site. This is the Golden Jubilee of the 1937 meeting at Manchester; it was the first on *Reaction Kinetics* and featured papers on potential-energy surfaces and transition-state theory by Henry Eyring, Michael Polanyi and Eugene Wigner. Also especially pertinent are the 1954 and 1979 meetings, both held here at Birmingham. I was still an undergraduate in 1954, but remember the excitement of my mentor in chemical kinetics, Harold Johnston, when he was invited to present a paper. A couple of years later, as a graduate student, I was intrigued to discover in the discussion volume the remarkable paper by Bull and Moon. This paper (which has notable neighbours, including contributions by Kistiakowsky, Norrish, Porter, Eigen . . .) described the bombardment of Cs vapour by a pulsed, accelerated  $\text{CCl}_4$  beam swatted by a high-speed rotor. My first Faraday Discussion came in 1962 at Cambridge, where I especially enjoyed talking with John Polanyi about molecular rotors in reactions. After five subsequent Discussions, we are both still spiraling about with high angular momentum! At the 1979 meeting, the Silver Jubilee of his swatting paper, I had the pleasure of meeting Prof. Moon and presenting work by Riley and Siska on alkali metal +  $\text{CCl}_4$  reactions which quantitatively confirmed his results. This also revealed rainbow structure in the product angle and energy distributions which indicated that the dynamics ‘involve spinning and swatting, much as in the apparatus of Bull and Moon’.

We are delighted that Prof. Moon is again with us. Knowing his fondness for versifying levity as well as levitating rotors, I want to offer these lines to renew our thanks for his bold experiment, literally the stuff that fables are spun of:

Hey, diddle, diddle: the carbon tet riddle,  
 The Bull whirled round with the Moon!  
 The little gas puffed to move so fast,  
 But the alkali speared it soon.  
 Alpha and beta, E-prime coupled theta,  
 Reaction urged by a harpoon.  
 A rainbow was left to show for it all,  
 And the salt ran away with the tune!

### Retrospect and Prospect

On looking back, however, what strikes me most about reaction dynamics as a field is the prevalence of centripetal rather than centrifugal evolution. Despite major advances

## Concluding Remarks

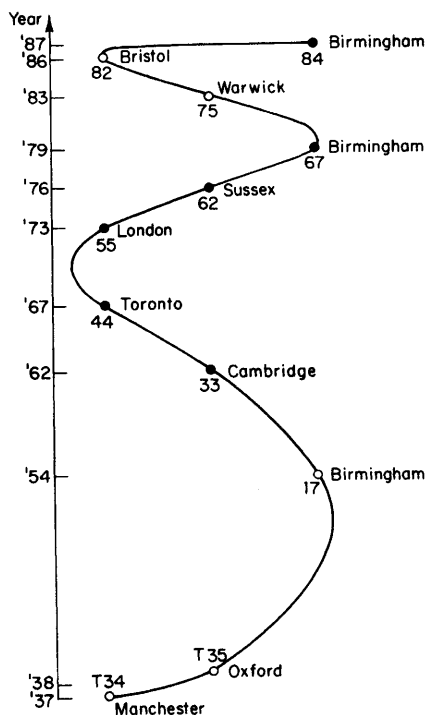


Fig. 1. Faraday discussions pertaining largely to reaction dynamics. Numbers labelling points indicate volume numbers (prefix T indicates *Trans. Faraday Soc.*).

in experimental/theoretical/computational repertoire and in chemical scope, this remains a cohesive, zestful field. Also striking among recruits new and old is an inviting sense of community, fostered both by the fundamental appeal of chemical dynamics and by expanding, uncrowded frontiers. This is indeed what Michael Polanyi envisioned in his essays, *The Republic of Science*<sup>1</sup> and *The Tacit Dimension*.<sup>2</sup>

The papers and posters at this Discussion exemplify three happy trends. (1) The *experimental* arena basks in the glow of an 'age of laser enlightenment'. New aspects include extending state-selection of reagents or analysis of products, particularly to ion-molecule reactions; providing versatile new beam sources for refractory materials; and enabling studies of reactive scattering of electronically excited atoms. (2) In the *collision theory* arena, classical trajectory, phase space, semiclassical and quantal scattering treatments are now much better integrated and implemented. For a given potential-energy surface, many dynamical properties can be reliably calculated. Frequently, two or three methods can be intercompared. The emphasis is on providing practical predictive or diagnostic results rather than theory swaddled in formalism. For instance, the reactive flux correlation function presented by Miller offers both a link to transition-state rate constants and a generic classification of reaction dynamics. (3) In the *electronic structure* arena, since potential-energy surfaces of requisite accuracy can as yet only be calculated for the simplest systems, more attention is being devoted to qualitative or semiquantitative concepts that can guide chemical interpretations of dynamical features. A prime example, lucidly treated by Dunning, is the concept of *reaction path*, so 'firmly embedded in the *lore* of chemistry'. Since only a swath across the potential surface need be computed, this approach is feasible for reactions involving four or more atoms. Like the reactive flux correlation function, the reaction path reaches back to the ancestral Manchester Discussion of fifty years ago.

Some vigorous subfields of reaction dynamics, absent or under-represented here, are discussed in other recent forms. These include laser *photodissociation*, the focus of a Faraday Discussion last year;<sup>3</sup> a broad and eclectic field now called dynamical stereochemistry or *stereodynamics*, treated at a Fritz Haber workshop in Jerusalem;<sup>4</sup> and the manifold dynamics of molecular *clusters* or van der Waals *complexes*, the subject of several recent conferences.<sup>5</sup>

Prospects are heartening for most parts of reaction dynamics. However, in these broad-brush benedictory comments I prefer to submit tacit optimism. This allows me to discuss briefly two specific topics that appear especially promising. Both involve angular momentum and literally bring new dimensions to reaction dynamics and to electronic structure.

### Angle–Angular Momentum Correlations

In effect, the potential-energy surface acts as a polarizing lens that induces anisotropies and correlations among the initial and final relative velocity and rotational angular-momentum vectors. Much of this dynamical information is seemingly lost by averaging over the random orientations of impact parameters and reactant molecules. That is why even single-collision experiments are not sufficient to characterize a potential surface, if limited to scalar properties such as energy distributions or to vector properties that depend on only a single angle, such as the product angular distribution. Yet in principle much of the information otherwise lost to the orientational averaging can be recovered from higher-order vector properties, termed *angular correlations*, that involve simultaneous measurement of two or more angles.

The pursuit of this ‘otherwise lost’ information comprises a chief theme of stereodynamics.<sup>6</sup> Our rather fitful progress has been reviewed elsewhere.<sup>7</sup> Unfortunately, the intimate analysis of angular momentum required for some aspects has caused many colleagues to complain that they are ‘certainly lost’. These colleagues will soon be rescued by a forthcoming text on angular momentum by Zare,<sup>8</sup> surely destined to be a canonical classic of chemical physics. Here I wish to examine two instructive questions pertaining to angle-angular momentum correlations. These stem from my paper with Kim at this meeting, but were held in reserve as deserving of emphasis in a wider context.

#### The Observability of an Unobservable Angle

Fig. 2 illustrates the *triple-vector correlation* among  $\mathbf{k}$ ,  $\mathbf{k}'$  and  $\mathbf{j}'$ , the initial and final relative velocities and the product rotational angular momentum, respectively. We have asserted that although the distributions of both  $\mathbf{k}'$  and  $\mathbf{j}'$  must have azimuthal symmetry about  $\mathbf{k}$ , when a subset is selected of  $\mathbf{k}'$  vectors with particular  $\mathbf{j}'$  (or *vice versa*), this subset in general will not have azimuthal symmetry about  $\mathbf{k}$ . Accordingly, the dihedral angle  $\phi$  between the  $\mathbf{k}$ ,  $\mathbf{k}'$  and  $\mathbf{k}$ ,  $\mathbf{j}'$  planes need not be uniformly distributed. A simultaneous measurement of two product vectors,  $\mathbf{k}'$  and  $\mathbf{j}'$ , would make  $\phi$  observable and thereby offer a means to undo the ‘dart-board’ averaging over the random azimuthal orientations of initial impact parameters. The quasiclassical trajectory calculations by Kim indeed show that the  $\phi$  distribution is a useful diagnostic property. The same situation will obtain for analogous angles in other vector correlations.<sup>6</sup>

In urging that  $\phi$  and other such neglected angles now serve as diagnostic properties, we meet the first of the two instructive questions. Is not  $\phi$  unobservable after all according to quantum mechanics? Only the magnitude and one projection of an angular momentum vector can be specified. Since we envision a measurement that specifies both the magnitude of  $\mathbf{j}'$  and the polar angle  $\chi$  between  $\mathbf{j}'$  and  $\mathbf{k}$ , the azimuthal angle about  $\mathbf{k}$  should be unobservable. That is so, for any particular measurement. But this

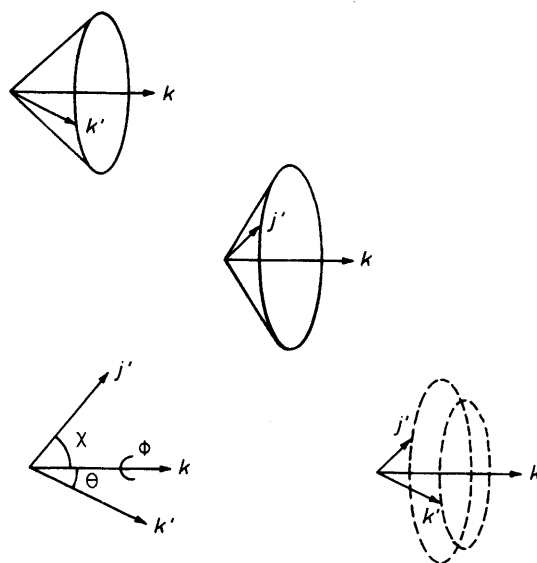


**Fig. 2.** Three-vector correlation among initial and final relative velocity vectors,  $k$  and  $k'$ , and product rotational angular momentum vector  $j'$ . Upper pair of diagrams indicate the azimuthal symmetry about  $k$  of the  $k'$  and  $j'$  vectors inherent when these are observed separately. Lower pair of diagrams indicates how the three-vector correlation can give information about the dihedral angle  $\phi$ , in effect undoing the azimuthal averaging about the initial relative velocity.

can be circumvented by measuring the angular momentum using several different choices for the axis of quantization. The data can then be combined to obtain moments of the  $\phi$  distribution as well as those of  $\chi$  and the scattering angle  $\theta$  between the  $k$  and  $k'$  velocity vectors.

The procedure<sup>6,9</sup> employs an expansion of the three-vector correlation in suitable orthogonal polynomials:

$$W(\theta, \chi, \phi) = \sum_{\nu\lambda\mu} A_{\nu\lambda\mu} P_{\nu\lambda\mu}(\theta, \chi, \phi). \quad (1)$$

This is just the generalization of the familiar expansion of a single-angle function in Legendre polynomials. The three-angle  $P_{\nu\lambda\mu}$  functions are rotationally invariant combinations of spherical harmonics; we have called them 'Biedenharn polynomials', to acknowledge a particularly lucid treatment of angular correlations.<sup>10</sup> The expansion coefficients  $A_{\nu\lambda\mu}$  characterize reaction stereodynamics in much the way that spectroscopic vibration-rotation parameters describe the force field of a molecule.

Eqn (1) is the classical version; the quantal version for any particular choice of quantization axis  $z$  corresponds to a uniform azimuthal average about the  $z$  direction. This does not affect  $\theta$ , which relates unquantized vectors, but replaces  $\chi$  and  $\phi$  by a single angle with cosine proportional to the  $j' \cdot z$  scalar product. The  $A_{\nu\lambda\mu}$  coefficients are unaffected by this average. Thus, once these are determined either from theory<sup>11</sup> or by combining experimental data taken with different choices of the  $z$  axis,<sup>12</sup> we can resurrect from eqn (1) the classical version of the three-vector correlation, including its  $\phi$  dependence. In this sense, quantum mechanics in effect allows a dihedral angle such as  $\phi$  to be observed even when the uncertainty principle does not permit this in any particular measurement.

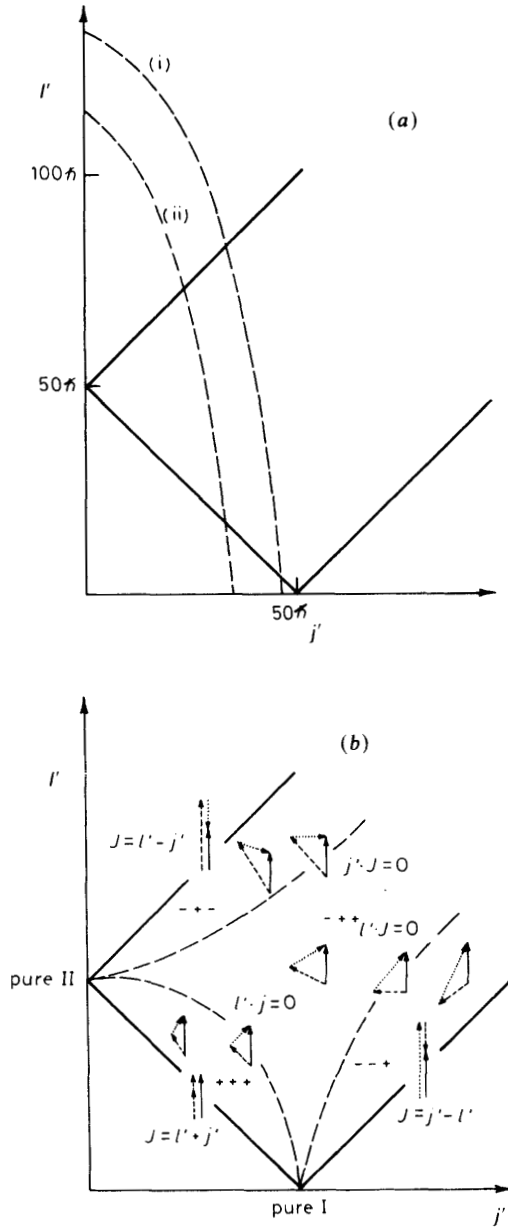


**Fig. 3.** Phase-space diagram for product angular momentum. (a) Straight lines indicate conservation constraints imposed by the triangle condition on the magnitudes:  $|l' + j'| > J |l' - j'|$ . Only points within the three-sided 'box' thus defined are allowed; for the case pictured,  $J = 50 \hbar$ . Dashed curves show energy constraint; outer curve (i) computed for no vibrational excitation of products ( $f_v = 0$ ), inner curve (ii) for most probable excitation ( $f_v = 0.4$ ). (b) Dashed solid lines define four regions defined by perpendicularity of the indicated pairs of vectors. These loci thus are determined from the Pythagorean theorem, which gives  $l'^2 = J^2 \pm j'^2$  and  $l'^2 = j'^2 - J^2$ . Inside each region are shown the signs of  $l' \cdot j'$ ,  $l' \cdot J$  and  $j' \cdot J$ , respectively, with corresponding orientations of  $J$  (solid),  $l'$  (dashed) and  $j'$  (dotted).

### A Kinematic Diagram for Angular Momentum Orientation

In the design and interpretation of single-collision experiments, analysis of the *kinematic* properties imposed by conservation laws has a key role. It provides means to recognize and evaluate features arising from the *dynamic* properties governed by the potential-energy surface. At the 1962 Discussion, a velocity vector diagram derived from conservation of energy and linear momentum was applied to the analysis of product angular distributions; this is referred to as a 'Newton Diagram'. Here we meet our second instructive question. How can we construct an analogous diagram from conservation of angular momentum for kinematic analysis of orientation angles?

Fig. 3 displays the components from which such a diagram may be assembled. For a fixed magnitude of the total angular momentum,  $J = l' + j'$ , the magnitudes of the exit orbital momentum and product rotational momentum correspond to points within a tilted, open-ended box defined by vector addition. The accessible portion of this box is defined by energy disposal.<sup>13</sup> If the reaction exoergicity and product vibrational excitation are specified, then the magnitudes of  $l'$  and  $j'$  are related by

$$Al'(l'+1) + Bj'(j'+1) = (1 - f_v)E_{\text{tot}} \quad (2)$$

where  $A$  is the reciprocal of  $2\mu'b^2/\hbar^2$ , involving the reduced mass of the product atom + diatom and the exit impact parameter,  $B$  is the rotational constant of the product molecule and  $f_v$  is the fraction of the available energy  $E_{\text{tot}}$  which appears in product vibrational excitation. In the phase-space theory it is customary to fix the  $A$  parameter by employing the venerable centrifugal barrier criterion.<sup>13</sup> The dashed lines shown in fig. 3(a) were obtained in this way for the H + Li<sub>2</sub> reaction. Other criteria will be more suitable in many cases;<sup>9</sup> the corresponding  $A$  parameters can readily be evaluated for any specified distribution of exit impact parameters.<sup>14</sup>

Within the domain of  $l', j'$  phase space allowed by conservation of angular momentum, there are four subdomains<sup>14</sup> that differ in the relative orientations of the  $J', l'$  and  $j'$  vectors. The dashed lines shown in fig. 3(b) define these regions. Since the energy constraint of fig. 3(a) imposes different weights on the four regions, by combining these diagrams we can obtain quick estimates for directional properties such as  $\langle l' \cdot j' \rangle$ . For instance, in the H + Li<sub>2</sub> case, we see that although there is cancellation between regions with  $l' \cdot j'$  positive and negative, the negative regions are dominant; hence  $l'$  and  $j'$  tend to be antiparallel, as found in Kim's trajectory study. For convenient reference, this useful combined diagram, fig. 3(a) and (b), needs a name. We suggest 'Holmes Diagram'. The immortal sleuth did in fact have some adventures with angular momentum,<sup>15</sup> and this centennial of his literary birth seems a good occasion to bestow on him honorary fellowship in the Royal Society of Chemistry.

### Dimensional Scaling for Electronic Structure

Virtually all *ab initio* electronic structure calculations now performed use the same basic method, the Hartree-Fock approximation (HF) plus configuration interaction (CI). The enormous growth in computing power has made feasible highly accurate HF calculations for many-electron systems, but the small residual error, termed the *correlation energy* (CE), remains recalcitrant because CI calculations are extremely arduous and slowly convergent. This is a crucial problem for reaction energies and often varies strongly with the geometrical configuration of the atoms. For instance, current calculations for the F + H<sub>2</sub> reaction employ millions of terms in the CI wavefunction but still have an error of ca. 30% in the activation energy.<sup>16</sup> Reliable means to predict activation energies, reaction intermediates and pathways could resolve myriad ambiguities in interpreting experiments and identifying reaction mechanisms.

Recently, we have explored a new approach using dimensional scaling methods.<sup>17-21</sup> Although so far fully implemented only for two-electron atoms, these methods offer

remarkably simple and accurate computational strategies for the correlation energy. Dimensional scaling also brings out novel heuristic concepts, including semiclassical features with uncanny links to the prequantum valence notions of Lewis and Langmuir.

The dimensional scaling approach has proved useful for many problems not amenable to ordinary perturbation methods, especially in statistical mechanics, particle and nuclear physics, and quantum optics. Typically the problem is solved analytically for some 'unphysical' dimension  $D=3$ , where the physics becomes much simpler, and then perturbation theory is employed to obtain an approximate result for  $D=3$ . Most often the analytic solution is obtained in the  $D \rightarrow \infty$  limit, and  $1/D$  is used as the perturbation parameter. In our study of the correlation energies for the ground state of two-electron atoms, we find the problem can be solved exactly in *two* limits,  $D \rightarrow \infty$  and  $D \rightarrow 1$ , and to a good approximation the CE is just a linear function of  $1/D$ . Linear interpolation between the exactly known limits gives total energies for  $D=3$  and  $Z \geq 2$  accurate to 0.005% or better, comparable to the best available configuration interaction calculations.

The Schroedinger equation is readily generalized to an arbitrary spatial dimensionality  $D$ , which denotes the number of Cartesian coordinates specifying the position vector for each electron relative to the atomic nucleus fixed at the origin. The Laplacian and Jacobian change form but not the potential energy.<sup>22</sup> For any central force problem, the radial Hamiltonian in  $D$ -dimensions is the same as for  $D=3$ , except that the orbital angular momentum  $l$  is replaced by  $\Lambda = l + \frac{1}{2}(D-3)$ . As noted long ago by Van Vleck,<sup>23</sup> in this case an isomorphism exists between angular momentum and dimensionality such that each half-unit increment in  $l$  is equivalent to a unit increment in  $D$ . For instance, the lowest  $P$  state for  $D=3$  corresponds to the lowest  $S$  state for  $D=5$ . For a hydrogenic atom, the ground-state energy is given by  $-\frac{1}{2}Z^2/\kappa^2$  hartree and the radial probability distribution has its maximum at  $\kappa^2/Z$  bohr, where  $\kappa = \frac{1}{2}(D-1)$ . Thus the energy vanishes as  $D \rightarrow \infty$  and becomes singular as  $D \rightarrow 1$ .

In treating other systems we use dimension-scaled units, proportional to the hydrogenic energy and distance, and thereby make the scaled energy finite in both limits. Likewise, we rescale the wavefunction to incorporate the square root of the  $D$ -dependent Jacobian volume element. This simplifies the Laplacian, explicitly displays the centrifugal potential, and reduces the Jacobian for the rescaled wavefunction to unity so that  $D$  may be varied with no further concern for implicit dimension dependence.

### Lewis Structures and Langmuir Vibrations

For large  $D$  the rescaled Hamiltonian for any atom or molecule takes a perspicuous form. It consists of kinetic-energy terms, all proportional to  $1/D^2$ , and an effective potential, independent of  $D$ , comprised of the rescaled centrifugal energy and the familiar Coulombic interactions. In effect, the factor  $\hbar^2/m_e$  involving Planck's constant and the electronic mass, which occurs in the unscaled kinetic energy, is replaced by  $1/D^2$  in the scaled version (whereas this factor cancels from the scaled centrifugal potential). The limit  $D \rightarrow \infty$  thus is tantamount to  $\hbar \rightarrow 0$  and/or  $m_e \rightarrow \infty$  in the kinetic energy. The electrons then assume fixed positions relative to the nuclei and each other which correspond to the minimum of the effective potential, the sum of the rescaled centrifugal and Coulombic terms. We call this the *Lewis structure*; it can be calculated exactly for any atom or molecule and provides a rigorous version of the qualitative electron-dot formulae introduced in 1916.

For  $D$  finite but very large, the electrons are confined to harmonic oscillations about the fixed positions attained in the  $D \rightarrow \infty$  limit. We call these motions *Langmuir vibrations*, in view of his prescient suggestion in 1919 that 'the electrons could . . . rotate, revolve, or oscillate about definite positions in the atom'. In the dimensional perturbation treatment the first-order term, proportional to  $1/D$ , corresponds to these harmonic vibrations, so the coefficient of this term is calculable from the curvatures of the effective

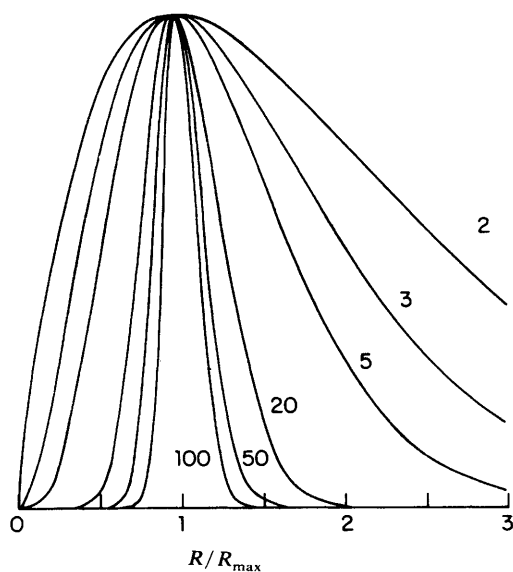


**Fig. 4.** Radial probability distribution for a ground-state hydrogenic atom in  $D$ -dimensional space. (Values of  $D$  are shown.) The curves are normalized at the maximum, which occurs at  $R_{\max} = [\frac{1}{2}(D-1)]^2/Z$ .

potential about its minimum. Accordingly, standard methods for normal mode analysis of molecular vibrations<sup>24</sup> become directly applicable to electronic structure.

### From Pseudoclassical Limit to Hyperquantum Singularities

The large- $D$  limit which emerges from dimensional scaling may be termed *pseudoclassical*, to indicate that it is not the same as the conventional classical limit obtained by  $\hbar \rightarrow \infty$  for a fixed dimension.<sup>25</sup> Since the unscaled centrifugal potential is proportional to  $\hbar^2$ , it does not contribute to the conventional limit. With dimensional scaling, however, the centrifugal term introduces barriers which prevent the electrons from falling into the nucleus, colliding with each other or finding the unstable trajectories<sup>26</sup> that exist when they are opposed by  $180^\circ$ . In short, adding 'extra' angular momentum as represented by  $D$  cures some major ills of the old quantum theory and thus invites use of modern semiclassical methods.

As  $D$  decreases further, the electron oscillations become increasingly anharmonic and change character from semiclassical to semiquantal. Eventually, for low  $D$  there occur the wild excursions corresponding to a strongly quantal domain. Fig. 4 illustrates for the hydrogen atom this progression in the radial distribution function. For two-electron atoms, the dependence on both  $D$  and  $Z$  has been mapped out by Loeser.<sup>18</sup> He generalized to arbitrary  $D$  both the Hylleras-Pekeris and Hartree-Fock algorithms, and thereby obtained very accurate ground-state total energies and correlation energies for a wide range of  $Z$  and for  $D = \infty$  down to below  $D = 1$ .

These results were complemented by an analysis of the low- $D$  regime by Doren.<sup>19</sup> The  $D \rightarrow 1$  limit is tantamount to  $\hbar \rightarrow \infty$  in the unscaled wave equation, hence represents a *hyperquantum* limit. Since the centrifugal potential disappears and the Coulombic interactions are replaced by delta functions,<sup>22</sup> this limit has an exact solution.<sup>27</sup> The dimension dependence is dominated by singularities at  $D = 1$ , arising from a second-order pole (like the hydrogenic atom but with a different residue) and a congruent



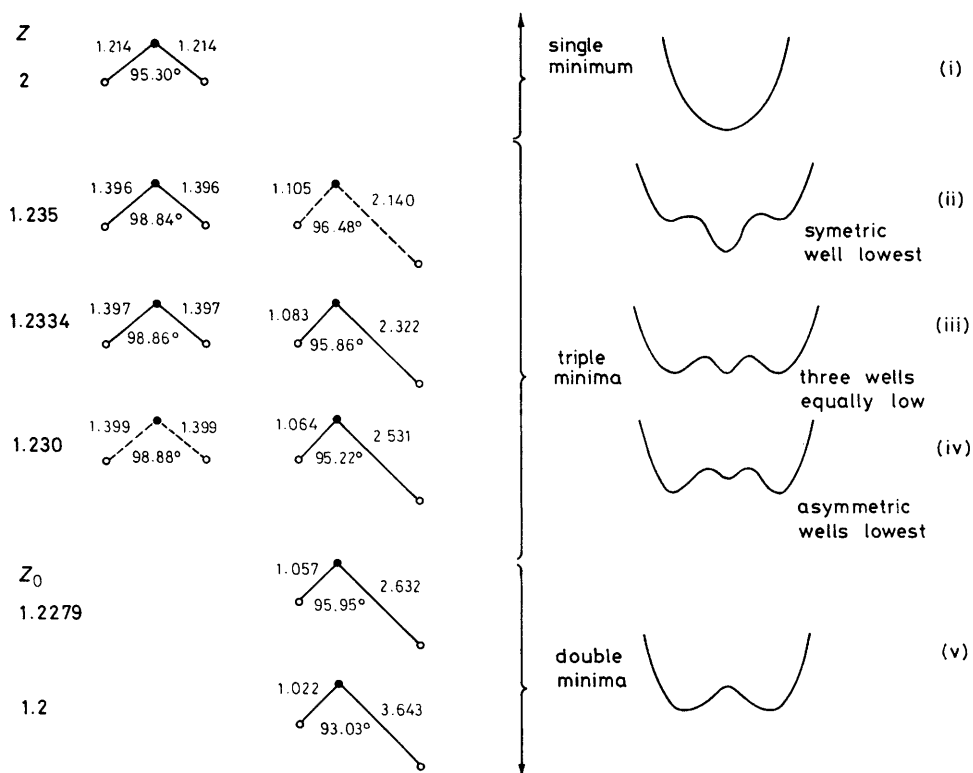


**Fig. 5.** Variation of Lewis structures ( $D = \infty$ ) for two-electron atoms in the symmetry breaking region (at left). Corresponding values of  $Z$ ,  $r_m$  and  $\theta_m$  are shown. Solid lines indicate structures that pertain to global minima, dashed those that pertain to less stable local minima as pictured schematically (at right): (i) single minimum; (ii) triple minima, symmetric well lowest; (iii) triple minima, three wells equally low; (iv) triple minima, asymmetric wells lowest; (v) double minima.

first-order pole. Deducting the readily calculable contributions from these poles markedly improves the efficacy of semiclassical dimensional perturbation expansions.

### Symmetry Breaking At Low $Z$ or Large $R$

The Lewis structure for helium and other two-electron atoms with  $Z \geq 2$  is symmetrical; the  $D \rightarrow \infty$  effective potential has a single minimum, with the electrons equidistant from the nucleus. The angle between the radii is obtuse rather than linear, since it reflects the competition between centrifugal repulsion (minimal at 90°) and interelectron repulsion (minimal at 180°). For helium this angle is  $\theta_m = 95.3^\circ$ , as compared to  $\cos^{-1}\{\cos \theta\} = 93.1^\circ$  for the  $D=3$  atom. However, when the nuclear charge drops below a critical value,  $Z_0 = 1.2279 \dots$ , the force constant for the antisymmetric stretching vibrational mode becomes negative. The symmetric configuration then becomes a saddle point, and the effective potential acquires two equivalent unsymmetrical minima that differ only by interchange of the electrons; these Lewis structures have one electron much closer to the nucleus than the other, as in the actual hydride ion. Fig. 5 shows how the electron geometry and the effective potential change in the transition region; for a short range just above  $Z_0$ , triple minima interpolate between the single and double minima regimes.<sup>28</sup>

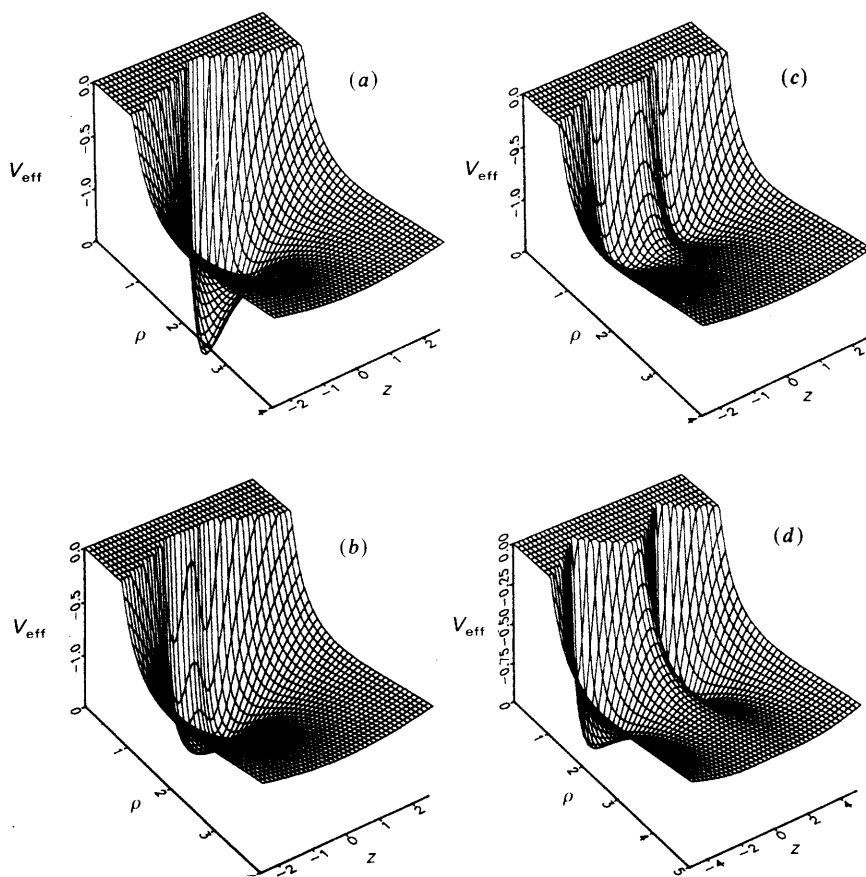


**Fig. 6.** Effective potential surfaces for the hydrogen molecule at  $D = \infty$  and various internuclear distances (bohr units),  $R$ : (a) 0, (b) 1, (c) 2 and (d) 3. These plots pertain to global minima, for which the electrons reside on a cylinder of radius  $\rho$  coaxial with the molecular axis ( $\rho_1 = \rho_2$ ), at equal distances  $z$  above and below the plane bisecting the nuclei ( $z_1 = -z_2$ ). The  $R = 0$  united atom limit pertains to helium and exhibits a single minimum corresponding to the symmetrical Lewis structure of fig. 6. Symmetry breaking occurs for  $R > ca. 0.9111$ , and a double minimum structure becomes increasingly pronounced for  $R = 1 \rightarrow 2 \rightarrow 5$ . Not evident are minor subsidiary minima (with  $z_1 = z_2$ ) in which both electrons are above or below the bisector plane.

This *symmetry breaking* transition, although confined to a narrow range of  $Z$ , has important repercussions elsewhere. It introduces a square-root branch point singularity in the zero-point energy of the Langmuir vibrations, which determines the coefficient of the first-order term in the  $1/D$  perturbation expansion. The effects of this singularity become particularly significant in the correlation energy. However, Loeser has found a satisfactory approximation which exploits the asymptotic character of the dimensional perturbation expansion.<sup>18,21</sup> This simply utilizes the  $1/D$  term up to the lowest non-vanishing order in  $1/Z$ ; as typically happens with asymptotic series, it turns out that 'less is more'.

In the Lewis structures for molecules, analogous symmetry-breaking transitions appear when either the nuclear charges or internuclear distances are varied. Fig. 6 shows effective potentials for the hydrogen molecule derived by Frantz.<sup>29</sup> When the separation  $R$  between the nuclei is small, the Lewis structure has the electrons in the

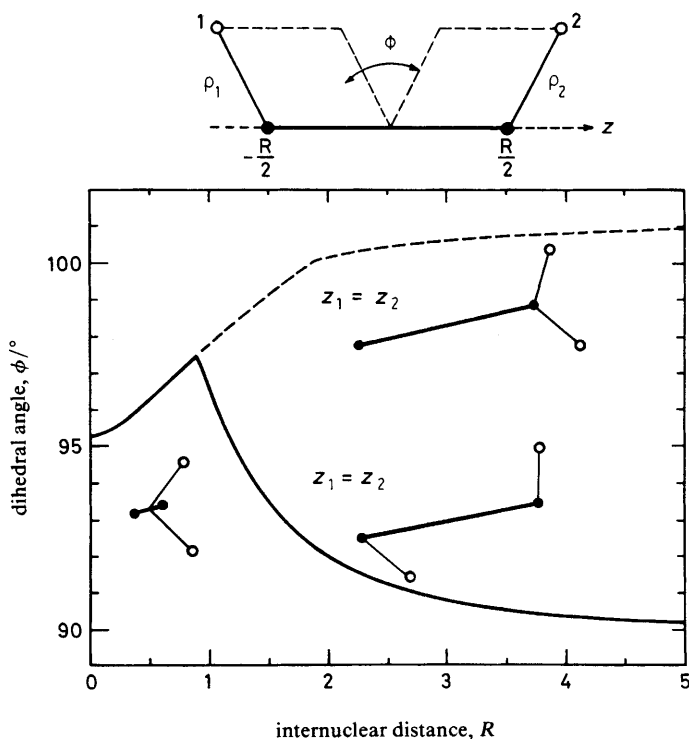


**Fig. 7.** Variation of dihedral angle for Lewis structures of hydrogen molecule with internuclear distance (bohr units). Symmetry breaking occurs at  $R \approx 0.9111$ , where  $\phi_m = 97.51^\circ$  and  $\rho_m = 0.9195$ ; stick figures show typical structures at smaller and larger  $R$ .

plane bisecting the molecular axis, but when  $R$  becomes large enough the potential acquires two pairs of double minima. One pair corresponds to localizing each electron on a different nucleus; the other pair, much less favourable energetically, has both electrons on one or the other nucleus. These ‘electronic isomers’ thus represent distinct valence bond structures. Fig. 7 gives another perspective, showing the dihedral angle (certainly unobservable!) between two planes hinged on the molecular axis, each containing one of the electrons. When viewed along the molecular axis, for small  $R$  the Lewis structure resembles that for the helium atom ( $R = 0$ ). As the critical internuclear distance is approached, the optimum dihedral angle opens up by a few degrees. At larger  $R$ , the dihedral angle decreases rapidly towards  $90^\circ$  for the most favourable structure (peroxide-like) but opens up further for the less favourable one (amino-like). It remains to be seen whether tracing out such features of these readily calculable Lewis structures will prove a useful complement to the traditional orbital pictures, but the prospect is inviting, particularly for analysis of electronic pathways in reactions.

### Overt Strategies and Hidden Virtues

At this early stage in applying dimensional scaling to electronic structure, the emphasis is on assessing possibilities. Most computations thus far have simply employed perturbation expansions in powers of  $1/D$ . In every case treated, when the hyperquantum and/or symmetry breaking singularities are taken into account, we find that even the first two terms (zero- and first-order), corresponding to the Lewis structure and Langmuir vibrations, give accuracy comparable to or better than the Hartree-Fock method. It appears

that treating electrons as if they were classical particles vibrating harmonically about fixed sites actually may provide as good a starting point for quantitative calculations as the conventional orbital description of wave mechanics.

The hydride ion provides a striking example, since restricted Hartree-Fock theory fails to predict the stability of the ground state. It is an extreme case: for  $D=3$ , only the ground state and the doubly excited  $2p^2\ ^3P^e$  state are bound, while for an infinitesimally larger nuclear charge, there are infinitely many bound states. Likewise, for  $D=\infty$  one of the electrons escapes into the ionization continuum. Doren found that the very simple first-order dimensional expansion, determined just from the hydrogenic contribution at  $D=\infty$  and the hyperquantum pole terms at  $D=1$  gives both bound states for  $H^-$  at  $D=3$  with an accuracy of a few tenths of a percent.<sup>28</sup> Both states are obtained in a single stroke, by virtue of an exact interdimensional degeneracy<sup>22</sup> between the excited state at  $D=3$  and the ground state for  $D=5$ . In this approximation, the poles at  $D=1$  are solely responsible for the stability of the atom, so much of the effect of short-range electron repulsion evidently is contained in the residues of those poles.

By augmenting the Lewis + Langmuir terms with insightful approximations, Loeser has devised an elegant and remarkably satisfactory treatment of  $N$ -electron atoms.<sup>21</sup> He greatly simplified the analysis by postulating that in the Lewis structure, the electrons are equidistant from one another and equidistant from the nucleus. Then the minimization of the effective potential involves only two free parameters, a single distance and a single angle, and the geometry and energy for  $D\rightarrow\infty$  are obtained from the smallest positive root of a quartic equation. The minimum puts the electrons at the corners of a regular  $N$ -point simplex, a 'hypertetrahedron', while the nucleus lies along an axis that passes perpendicularly through the centroid. Prof. G. N. Lewis would surely be delighted at this generalization of his cubical atom!

To take account of the Pauli principle, Loeser assumed that the spin and symmetry rules are unaltered in  $D$ -space and related the various Langmuir vibrational modes to the familiar electron configurations  $|n_1 l_1 \dots n_N l_N\rangle$  in the double limit  $D, Z \rightarrow \infty$ , where both representations become exact. Also, as already noted, to avoid or reduce contributions from symmetry-breaking transitions, Loeser deleted terms beyond the lowest nonvanishing order in  $1/Z$  from the Langmuir vibrations. In this way he obtained total energies with maximum errors of only *ca.* 1%, for atoms with up to  $N \approx 100$  electrons. In subsequent work Loeser has found calculations at the same order of approximation yield correlation energies that agree to within the estimated uncertainties with most known values.

From our current perspective, dimensional scaling offers two promising computational strategies for correlation energies. One route is to use the HF method in the conventional way but to supplement or replace the CI calculations by a  $1/D$  expansion to evaluate the CE corrections.<sup>18</sup> This relies on the fact that in the limiting cases (pseudoclassical and hyperquantum) used to construct the perturbation expansion, the complete Hamiltonian is solved. The ability of the expansion to represent the  $D=3$  solution thus does not depend on the magnitude of the interaction but only on its dimension dependence. For multielectron systems, the location of the important hyperquantum singularities will not be evident beforehand. However, Goodson has developed a powerful moment method<sup>20</sup> for computing to high accuracy the perturbation coefficients of the  $1/D$  series. With this he has recently evaluated the coefficients for helium to 20 significant figures, up to order 15. Since the power series itself is asymptotic, it is not directly useful. However, Padé approximants constructed from the coefficients yield extremely accurate energies (as well as the location and residues of the hyperquantum poles).

The other dimensional scaling strategy aims to improve the HF approximation and thereby reduce the magnitude of the CE correction. As with the analogous mean-field approximation in statistical mechanics, the correlation error in the HF method is expected

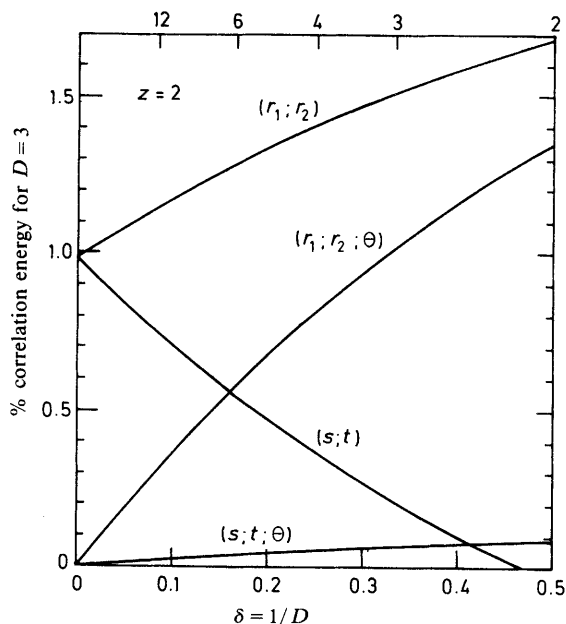


**Fig. 8.** Approximate correlation energies (as percentage of total energy) for the ground-state helium atom as functions of  $\delta = 1/D$ , for four choices of separable 'modified Hartree-Fock' wavefunctions ( $z = 2$ ). Each is constructed from factors that depend on a single coordinate, as indicated. The coordinates denoted by  $s$  and  $t$  are proportional to  $r_1 \pm r_2$ , respectively. The result for normal-coordinate separation ( $q_1; q_2; q_3$ ) coincides with abscissa axis. (a)  $(r_1; r_2)$ , (b)  $(r_1; r_2; \theta)$ ; (c)  $(s; t)$ , (d)  $(s; t; \theta)$ .

to diminish as  $D$  increases. This is because fluctuations decrease in proportion to  $D^{-1/2}$ , as illustrated in fig. 4 for the H atom. However, whereas the mean-field approximation for critical exponents of phase transitions becomes exact for sufficiently large  $D$ , for the HF approximation the CE remains non-zero and relatively large even for  $D \rightarrow \infty$ . As a function of the total energy, the CE for the helium atom varies from 2.3% at the  $D \rightarrow 1$  limit to 1.5% for  $D = 3$  to 0.99% at the  $D \rightarrow \infty$  limit.

The origin of this large residual CE at the  $D = \infty$  limit is evident from the dimensional perturbation treatment. The HF wavefunction, constructed as a product of one-electron orbitals, lacks any explicit dependence on the angle  $\theta$  between the electron radii. Hence this angle enters only in the Jacobian volume element, which contains  $(\sin \theta)^{D-2}$ ; therefore as  $D \rightarrow \infty$ , the angle becomes fixed at  $90^\circ$ . The corresponding Lewis structure is in error simply because this constraint on the angle does not allow the HF method to find the correct minimum of the effective potential, which has  $\theta_m = 95.3^\circ$ .

The correlation error at  $D \rightarrow \infty$  can be made to vanish by modifying the HF variational wavefunction, as shown by Goodson in another study.<sup>20</sup> It is only necessary to introduce an explicit dependence on  $\theta$ , and this can be done while retaining a separable form for the wavefunction. Likewise, the error in the HF value for the first derivative of the energy with respect to  $1/D$  can be made to vanish. This involves using as coordinates the normal modes  $q_i$  for the Langmuir vibrations. By thus eliminating the large HF error for the  $D \rightarrow \infty$  limit, the CE for  $D = 3$  will be markedly reduced. Fig. 8 shows estimates obtained by Goodson for the dimension dependence of the correlation energies corresponding to various coordinate choices in such modified HF functions.

Aside from enhancing computational methods and heuristic concepts, dimensional scaling also answers a persistent philosophical question of quantum theory: might not

'hidden' classical variables exist despite the uncertainty principle? The pseudoclassical limit shows that such variables do exist, for  $D \rightarrow \infty$ . Although this limit yields equations entirely classical in form, it is nonetheless consistent with the uncertainty principle.<sup>17</sup> Scaling the coordinates in proportion to  $D^2$  implies that the conjugate momenta are scaled inversely, so the commutators and the uncertainty principle remain invariant. In effect, the dimensional scaling brings out the underlying classical structure and hides the quantum mechanics. Our seemingly classical calculations of the Lewis and Langmuir terms are still fully quantum-mechanical. This is a fundamental reason why dimensional scaling gives surprisingly good results.

The underlying motif of fig. 1 is a spiral of understanding. Our successors will likewise return repeatedly (like Prof. Moon's spinning rotors) to fundamental themes in the molecular dynamics of reactions. With this in mind, these closing remarks are really intended as opening remarks for the next upward spiral. We now recognize that previously neglected 'unobservable' angles in reaction stereodynamics and 'unphysical' dimensions in electronic structure offer new insights and a new calculus. Both provide welcome tools for forging higher spiral links. Both also reveal a deeper role than previously suspected for classical mechanics within quantum mechanics. This is an apt turn of affairs in the tercentenary year of the publication of Newton's *Principia*.

## References

- 1 M. Polanyi, *Minerva*, 1962 **1**, 54.
- 2 M. Polanyi, *The Tacit Dimension* (Doubleday, New York, 1966).
- 3 R. N. Zare, *Faraday Discuss. Chem. Soc.*, 1986, **82**, 391.
- 4 See papers in *Dynamical Stereochemistry*, ed. R. D. Levine, *J. Phys. Chem.*, 1987, **91**.
- 5 See *Structure and Dynamics of Weakly Bound Molecular Complexes*, ed. A. Weber (Reidel, Boston, 1987); *Metal Clusters*, ed F. Trager and G. zu Putlitz, *Z. Phys., Teil D*, 1986, **3**; R. Naaman, *Adv. Chem. Phys.*, 1987, in press.
- 6 J. D. Barnwell, J. G. Loeser and D. R. Herschbach, *J. Phys. Chem.*, 1983, **87**, 2781.
- 7 R. B. Bernstein, D. R. Herschbach and R. D. Levine, *J. Phys. Chem.*, 1987, **91**, 5365.
- 8 R. N. Zare, *Angular Momentum in Quantum Mechanics* (Wiley, New York, 1988).
- 9 D. A. Case and D. R. Herschbach, *Mol. Phys.*, 1975, **30**, 1537.
- 10 L. C. Biedenharn, in *Nuclear Spectroscopy, Part B*, ed. F. Azjenberg-Selove (Academic Press, New York, 1960), p. 732.
- 11 G. M. McClelland and D. R. Herschbach, *J. Phys. Chem.*, 1987 **91**, 5509.
- 12 D. A. Case, G. M. McClelland and D. R. Herschbach, *Mol. Phys.*, 1978, **35**, 541.
- 13 J. C. Light, *Faraday Discuss. Chem. Soc.*, 1967, **62**, 1372 and work cited therein.
- 14 D. A. Case and D. R. Herschbach, *J. Chem. Phys.*, 1976, **64**, 4212.
- 15 See especially, A. C. Doyle, *The Musgrave Ritual*, in *The Memoirs of Sherlock Holmes* (Harper & Brothers, London, 1894). I thank Prof. R. N. Zare for this reference.
- 16 H. Jafee (work in progress, Ames Laboratory, Moffit Field, California).
- 17 D. R. Herschbach, *J. Chem. Phys.*, 1986, **84**, 838.
- 18 J. G. Loeser and D. R. Herschbach, *J. Phys. Chem.*, 1985, **89**, 3444; *J. Chem. Phys.*, 1986, **84**, 3882; 3903; 1987, **86**, 2114; 3512.
- 19 D. J. Doren and D. R. Herschbach, *Chem. Phys. Lett.*, 1985, **118**, 115; *Phys. Rev. A*, 1986, **34**, 2654, 2665; *J. Chem. Phys.*, 1986, **85**, 4557; 1987, **87**, 433.
- 20 D. Z. Goodson and D. R. Herschbach, *Phys. Rev. Lett.*, 1987, **58**, 1628; *J. Chem. Phys.*, 1987, **86**, 4997.
- 21 J. G. Loeser, *J. Chem. Phys.*, 1987, **86**, 5635.
- 22 D. R. Herrick and F. H. Stillinger, *Phys. Rev., Part A*, 1975, **11**, 42.
- 23 J. H. Van Vleck, in *Wave Mechanics, the First Fifty Years* (Butterworths, London, 1973), pp. 26–37.
- 24 E. B. Wilson, J. C. Decius and P. C. Cross, *Molecular Vibrations* (McGraw-Hill, New York, 1955).
- 25 L. G. Yaffe, *Rev. Mod. Phys.*, 1982, **54**, 407.
- 26 G. H. Wannier, *Phys. Rev.*, 1953, **90**, 817.
- 27 C. M. Rosenthal, *J. Chem. Phys.*, 1971, **55**, 2474.
- 28 D. J. Doren and D. R. Herschbach, *J. Phys. Chem.*, 1988, in press.
- 29 D. J. Frantz and D. R. Herschbach, *Chem. Phys. Lett.*, 1988, in press.